

promoting access to White Rose research papers



Universities of Leeds, Sheffield and York
<http://eprints.whiterose.ac.uk/>

This is an author produced version of a paper published in **Physical Review B**.

White Rose Research Online URL for this paper:

<http://eprints.whiterose.ac.uk/42649>

Published paper

Makhonin, M.N., Chekhovich, E.A., Senellart, P., Lemaitre, A., Skolnick, M.S., Tartakovskii, A.I. (2010) *Optically tunable nuclear magnetic resonance in a single quantum dot*, Physical Review B, 82 (16), Article no.161309

<http://dx.doi.org/10.1103/PhysRevB.82.161309>

Optically tunable nuclear magnetic resonance in a single quantum dot

M. N. Makhonin¹, E. A. Chekhovich^{1,2}, P. Senellart³, A. Lemaître³, M. S. Skolnick¹, A. I. Tartakovskii¹

¹ *Department of Physics and Astronomy, University of Sheffield, S3 7RH, UK*

² *Institute of Solid State Physics, RAS, Chernogolovka, 142432, Russia,*

³ *Laboratoire de Photonique et de Nanostructures, Route de Nozay, 91460 Marcoussis, France*

(Dated: November 16, 2010)

We report optically detected nuclear magnetic resonance (ODNMR) measurements on small ensembles of nuclear spins in single GaAs quantum dots. Using ODNMR we make direct measurements of the inhomogeneous Knight field from a photo-excited electron which acts on the nuclei in the dot. The resulting shifts of the NMR peak can be optically controlled by varying the electron occupancy and its spin orientation, and lead to strongly asymmetric lineshapes at high optical excitation. The all-optical control of the NMR lineshape will enable position-selective control of small groups of nuclear spins inside a dot.

Nuclear spins offer a nano-scale resource with extended spin life-times and coherence, leading to proposals to use nuclei for quantum computation [1–4] and coherent spin-memories [5]. Strong interest in nuclear spin effects in semiconductors has also been recently stimulated by research into manipulation of single spins in nanostructures, where the electron-nuclear (hyperfine) interaction plays an important role [6–8]. Direct control of nuclear spins by resonant techniques such as NMR is highly desirable for both electron and nuclear spin manipulation experiments. In the past NMR methods have been widely applied to large volume semiconductor structures (bulk, heterojunctions, quantum wells etc) containing very large number of nuclei in the range 10^8 or significantly more [4, 9–13]. Further refinement of these methods has made it possible to detect magnetic resonance of as few as 10^4 nuclei in otherwise abundant spin environments by detecting the optical response from individual GaAs quantum dot nano-structures in micro-photoluminescence experiments [14, 15]. These micro-ODNMR experiments revealed strong dot-to-dot variation of resonant frequencies [16], arising from interaction of small nuclear spin ensembles with random Knight fields from single spins of localized electrons [17].

In this work we take advantage of the strong gradients of the Knight field inside a quantum dot produced by the localized electron spin and enter a new regime of *nano*-ODNMR. By employing ODNMR techniques first reported in Refs.[14, 15], we measure with high precision the Knight shifts in the resonant frequencies of each individual isotope spin sub-system in individual GaAs/AlGaAs interface dots and find their dependence on the polarization and power of optical excitation. By varying the optical power, we find striking modifications of the lineshape of the NMR spectrum of the dot. These arise from the Knight field variation across the dot determined by the spatial distribution of the electron wavefunction. The interpretations are supported by calculations, which further demonstrate that by employing the inhomogeneities of the Knight shifts, it becomes possible to access selectively, by appropriate resonant frequencies,

small groups of nuclear spins located in different regions within the dot (hence the term nano-ODNMR). This may be used for spatially-selective control of the nuclear spins in nanometer-sized semiconductor structures.

The dependence of the NMR frequencies on the intensity and polarization of optical excitation arises from the optically-induced Knight field, B_e , a result of the contact hyperfine interaction between an individual nuclear spin and an electron confined in the dot [18–20]. In an uncharged dot, as in our case, B_e arises from the photo-excited electrons, with the time-averaged dot occupancy, F , and mean electron spin polarization ρ , controlled by the intensity and polarization of light, respectively. The time-averaged magnitude of the Knight field for a nucleus with a hyperfine constant A at the position \mathbf{r} depends on the nuclear gyromagnetic ratio γ and is given by [18]:

$$B_e = -\frac{v_0 A}{\hbar \gamma Z} |\psi(\mathbf{r})|^2 \rho F \quad (1)$$

Here v_0 is the volume of the crystal unit cell, containing $Z = 4$ Ga or As nuclei, and $0 \leq \rho \leq 1$ and $-1 \leq \rho \leq 0$ for the electron with spin up and down, respectively. B_e follows the distribution of the electron envelope function $\psi(\mathbf{r})$ in the dot leading to the nuclear site-dependent field varying across the dot. In what follows the corresponding site-dependent Knight shifts in the NMR frequency given by $\Delta f = \gamma B_e / 2\pi$ are measured with high precision in individual QDs.

The sample investigated contains interface QDs formed naturally by 1 monolayer width fluctuations in a nominally 13 monolayer GaAs layer embedded in $\text{Al}_{0.33}\text{Ga}_{0.67}\text{As}$ barriers (see growth details in Ref.[21]). In contrast to self-assembled quantum dot structures, interface dots are formed by lattice-matched GaAs and AlGaAs layers, leading to reduced strain and weak quadrupole effects, resulting in narrow NMR linewidths. This makes the interface dots an ideal test bed for future applications of ODNMR in III-V semiconductor nanostructures. Knight field effects detected by ODNMR are observable in a wide range of magnetic fields. By contrast, all-optical detection based on compensation of B_e

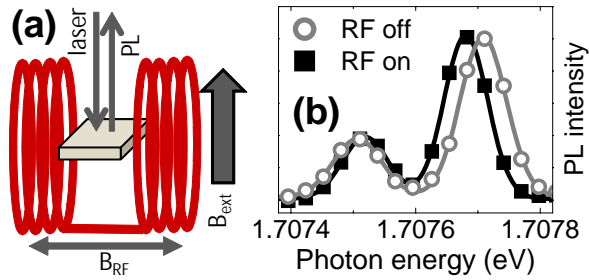


FIG. 1: (color online). (a) Diagram of the ODNMR experiment, depicting optical excitation and PL collection in the Faraday geometry, and the in-plane B-field B_{RF} oscillating at a radio frequency. (b) PL spectra of the neutral exciton in a GaAs dot with and without RF excitation (squares and circles, respectively) at $B_{ext} = 2T$. Lines show results of the peak fitting.

by external magnetic fields is only possible at very low fields in the mT range [19, 20].

The ODNMR setup is sketched in Fig.1a. External magnetic field B_{ext} is applied in the Faraday geometry. Optical excitation is used for (i) pumping the nuclear spin via dynamic nuclear polarization (DNP)[14, 15, 19, 20, 20, 22–25] and (ii) to excite photoluminescence (PL) for measurements of the exciton Zeeman splittings in individual dots. The measurements were carried out at a temperature $T = 4.2$ K. We use an excitation laser at 670 nm which generates electrons and holes in the quantum well (QW) states ≈ 130 meV above the QD emission lines. PL was detected with a double spectrometer and a charge coupled device. As shown in Fig.1a, a coil was wound around the sample for RF excitation of the dots. The coil was excited by the output from a radio frequency (RF) generator and provided transverse magnetic fields B_{RF} up to 0.6 Gauss.

We study neutral dots. Fig.1b shows exciton PL spectra [23] measured for $B_{ext} = 2T$ under σ^+ polarized laser excitation with and without RF excitation (squares and circles, respectively). The two peaks observed in the spectrum belong to the exciton Zeeman doublet. Excitation with circularly polarized light results in the pumping of nuclear spins in the dot and gives rise to the Overhauser field B_N [14, 15, 19, 20, 22–25]. B_N is detected through the resulting change in the exciton Zeeman splitting, $\Delta E_{XZ} = g_e \mu_B B_N$ [g_e electron g-factor, μ_B - Bohr magneton, B_N is co-(anti-) parallel to B_{ext} for σ^- (σ^+) excitation]. Using lineshape fitting ΔE_{XZ} is measured with an accuracy of $\approx 1 \mu eV$. RF excitation resonant with nuclear spin transitions in any of the three isotope subsystems contained in the dot (^{75}As , ^{71}Ga , ^{69}Ga [14, 15]) leads to nuclear spin depolarization and consequent reduction of $|B_N|$. This is observed in Fig.1b as a change in the splitting of the Zeeman doublet when RF excitation is applied. In what follows we will use the variation of the exciton Zeeman splitting upon optical or RF exci-

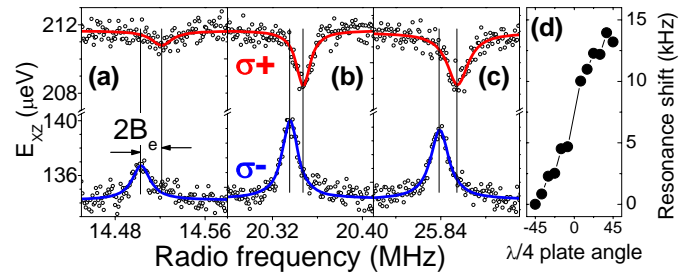


FIG. 2: (color online). Symbols show NMR spectra $E_{XZ}(f_{RF})$ measured at moderate optical power of $0.5 \mu W$ at $B_{ext} = 2T$ for ^{75}As (a), ^{69}Ga (b), ^{71}Ga (c). Data obtained with $\sigma^{+(-)}$ excitation are fitted with the red (blue) line. Vertical lines mark positions of the NMR peaks. (d) Shift of the resonance frequency for ^{69}Ga as a function of the rotation angle of the $\lambda/4$ plate in the laser excitation path.

tation to measure changes in the nuclear polarization in the dot.

Fig.2 shows NMR spectra $E_{XZ}(f_{RF})$ for ^{75}As , ^{69}Ga , ^{71}Ga at $B_{ext} = 2T$ recorded under simultaneous RF and circularly polarized laser excitation (a moderate pumping power, P of $0.5 \mu W$ is employed, corresponding to $F \approx 0.1$). The spectra exhibit peaks and dips for σ^- and σ^+ excitation, respectively, with a typical width of ≈ 15 kHz. Fig.2 shows a strong dependence of the resonance frequency on the polarization of optical excitation [17]. A change of the laser polarization leads to the change in the time-averaged electron spin polarization ρ in Eq.1. When the polarization is tuned from σ^+ to σ^- , the resonance frequency is also tuned gradually as shown in Fig.2d. The total frequency shift between the resonances measured for σ^+ and σ^- excitation corresponds to twice the maximum average Knight field $2B_e^{max}$ for a given optical power for nuclei of a particular isotope. For the moderate excitation power used in this experiment the following magnitudes of B_e^{max} were found: $B_e(^{75}As) = 1mT$, $B_e(^{69}Ga) = 0.57mT$ and $B_e(^{71}Ga) = 0.62mT$. The above magnitudes of the Knight field are comparable with those reported for InGaAs QDs [19] ($< 1mT$) and somewhat smaller than up to 3 mT observed in InP dots [20]. Each individual field magnitude reported in Fig.2 is at least an order of magnitude larger than was reported for GaAs/AlGaAs QWs [12], due to the stronger localization of the electron in quantum dots.

We will now demonstrate the effect of electron occupancy F (see Eq.1), increasing with the optical power, on the nuclear magnetic resonance frequency. Fig.3 shows NMR spectra recorded for ^{71}Ga at $B_{ext} = 1.99$ T using continuous RF and optical excitation. The vertical lines and arrows at 25.822 MHz in (a) and (b) show the peak positions of NMR spectra measured in the "dark" using pulsed techniques, where the laser is switched off during the RF excitation leading to $B_e = 0$ [26]. Fig.3a shows NMR spectra measured for different powers of σ^+ polar-

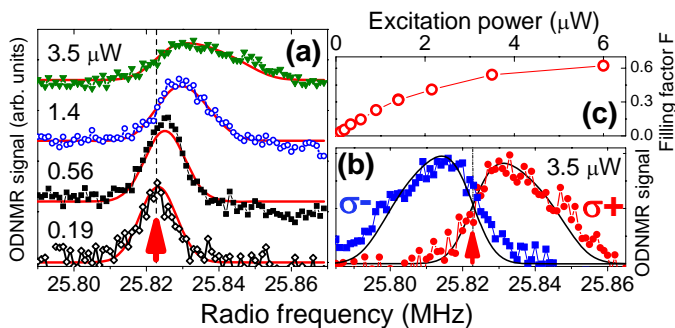


FIG. 3: (color online). Symbols in (a) and (b) show NMR spectra $\Delta E_{XZ}(f_{RF})$ for ^{71}Ga measured at $B_{ext} = 1.99\text{T}$. (a) data for powers 0.19, 0.56, 1.4 and $3.5 \mu\text{W}$ of σ^+ polarized light. (b) data for σ^+ and σ^- polarized light with power $3.5 \mu\text{W}$. Lines show fitting obtained using Eq.2 for a dot with the height of 4 nm and diameter 40 nm for $\rho = 0.3$ and F of 0.05, 0.14, 0.32 and 0.54 in (a) and $F = 0.54$ in (b). Arrows and dotted vertical lines in (a) and (b) indicate peak position of the NMR spectra measured in the dark for $B_e = 0$ [26]. (c) Power dependence of F obtained from the fitting.

ized light. A peak shift from the line corresponding to $B_e = 0$ is observed, which increases from 1 kHz for 0.19 μW excitation power to 8 kHz for 3.5 μW . In addition to the shift there is a strong modification of the lineshape: the full width at half maximum changes from 12 kHz at 0.19 μW to 27 kHz at 3.5 μW . A pronounced asymmetry of the NMR spectrum is also observed at 3.5 μW on the high frequency side of the spectrum. As expected, the form of this asymmetry is strongly dependent on the polarization of optical pumping. Fig.3b illustrates this with two NMR spectra recorded under σ^+ and σ^- polarized excitation at an optical power of 3.5 μW . In contrast to the case of σ^+ pumping, the spectrum measured with σ^- excitation is strongly broadened towards lower frequencies, corresponding to occurrence of a high negative Knight field.

In order to analyze the effect of the inhomogeneous Knight field quantitatively we have calculated the distribution of the NMR frequencies in an ensemble of nuclei in a dot under optical excitation. The position-dependent frequency shifts are calculated using Eq.1 and can be expressed as $\Delta f(\mathbf{r}) = -\frac{v_0}{\hbar Z} |\psi(\mathbf{r})|^2 A_i \rho F$. In GaAs $A_{As} = 5.69\text{GHz}$, $A_{69Ga} = 4.66\text{GHz}$ and $A_{71Ga} = 6.00\text{GHz}$. For the spin ensemble of ^{71}Ga (data in Fig.3) we use an experimentally observed Gaussian distribution of frequencies for an empty dot $F = 0$ [i. e. $\Delta f(\mathbf{r}) = 0$] with central frequencies of $f_0 = 25.822\text{ MHz}$ for $B_{ext} = 1.99\text{T}$, and a finite width $w_0 = 12\text{kHz}$ most probably originating from weak residual strain. Under optical excitation, at a given radio frequency the response of the nuclei in the dot will be described with a Gaussian distribution where f_0 is replaced by the position-dependent $f_0 + \Delta f(\mathbf{r})$.

The Overhauser shift, ΔE_{XZ} , observed in the experiment is a result of contributions from all nuclei in the dot.

However, the contribution of individual nuclei is dependent on the strength of the hyperfine interaction with the optically excited electron, and is therefore proportional to $|\psi(\mathbf{r})|^2$. In the ODNMR experiment we measure the reduction in $|\Delta E_{XZ}|$ as a result of the interaction with RF excitation at a given frequency. Such depolarization of the nucleus at the position \mathbf{r} will be observed at the resonant condition $f = f_0 + \Delta f(\mathbf{r})$. Thus $|\Delta E_{XZ}(f)|$ can be calculated by integration over the volume of the dot:

$$|\Delta E_{XZ}(f)| \propto \int |\psi(\mathbf{r})|^2 \exp[-(f - f_0 - \Delta f)^2 / 2w_0^2] d^3r \quad (2)$$

The results of these calculations are shown in Fig.3 by the full lines. Here parameter ρ in Eq.1 is ≈ 0.3 as found from the degree of circular polarization in PL spectra. In the fitting procedure we also assume that $F \propto I_{PL}$, the PL intensity measured in experiment. For this model calculation we use a cylindrical GaAs/Al_{0.3}Ga_{0.7}As dot. For calculations of the electron wave-function the dimensions of the dot are crucially important parameters. As the Knight field B_e is proportional to $|\psi(\mathbf{r})|^2$ with the normalization condition $\int |\psi(\mathbf{r})|^2 d^3r = 1$, B_e is inversely proportional to the characteristic volume of the electron wave-function V_{wf} , defined in turn by the volume of the dot. We fix the size of the dot (and hence the form of the wave-function and V_{wf}), and then find F by fitting the NMR data. In our case, the dot height of 4 nm is given by the thickness of the GaAs quantum well. The fitting shown in Fig.3 is obtained for the dot diameter $D = 40\text{ nm}$, a size close to that used in previously reported calculations [27]. As F and $|\psi(\mathbf{r})|^2$ enter the expression for B_e (Eq.1) as a product, it follows that the fitting results for data in Fig.3 depend on the ratio F/V_{wf} . Since V_{wf} is roughly proportional to D^2 , by increasing (decreasing) D by a factor ν , from the fitting we obtain magnitudes of F increased (decreased) by a factor of $\approx \nu^2$, as verified by simulations for different dot sizes (not shown).

As I_{PL} saturates at high power, the magnitude of F obtained from the fitting in Fig.3 increases sub-linearly with power as shown in Fig.3c: it is 0.05 for 0.19 μW , 0.14 for 0.56 μW , 0.32 for 1.4 μW , and 0.54 for 3.5 μW in Fig.3a. In the regime where exciton PL starts to saturate the fitting yields a reasonable $F \approx 0.5$ [28].

The strong electron confinement leads to strong gradients of the Knight field in the dot. To illustrate this point, Fig.4 shows the calculated Knight shift as a function of the in-plane distance r (Fig.4a) and vertical coordinate z (Fig.4b) from the position of the maximum of the electron wave-function. In what follows the calculations have been carried out for a dot with 40 nm diameter (i.e. the wave-function as in the fitting above). We will also describe the calculated curves in terms of the product ρF as it enters in the definition of B_e in Eq.1.

In Figs.4a,b $\rho F = 0.2$ close to the maximum obtained in the fitting in Fig.3. The vertical bar in Fig.4b shows for

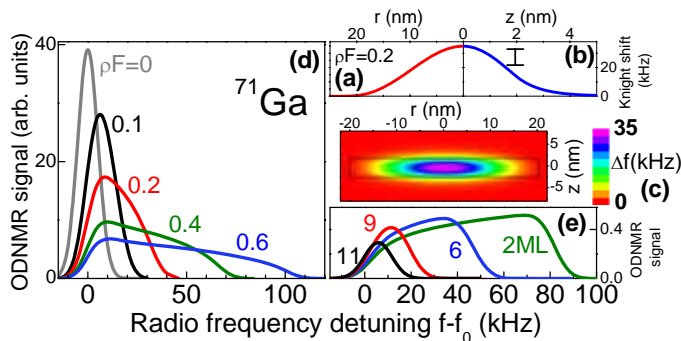


FIG. 4: (color online). The Knight shift of ^{71}Ga as a function of the in-plane distance r (a) and vertical coordinate z (b) from the maximum of the electron wave-function for the case $\rho F = 0.2$. (c) The distribution of the Knight shift in the ^{71}Ga nuclear spin ensemble in the dot of 4 nm height and 40 nm diameter. The scale for Δf is shown opposite. The graph depicts a vertical cross-section through the middle of the dot (the dot boundaries are shown by black lines). (d) NMR curves calculated for ^{71}Ga in the dot using Eq.2 for different magnitudes of ρF . (e) NMR curves calculated for $\rho F = 0.5$ for a mono-layer of ^{71}Ga displaced vertically from the center of the dot by 2, 6, 9 and 11 mono-layers.

comparison the width w_0 of the ^{71}Ga resonance without the influence of the optically excited electron (the case of $F = 0$). As seen from the plots, the presence of the electron perturbs the resonance frequency distribution in a major way, leading to strong gradients in both in-plane and vertical directions: the resonance frequency changes by more than w_0 on a 10 nm length-scale in-plane and in 2 nm in the z -direction. This opens up the possibility for nano-ODNMR - high spatial selectivity in addressing small groups of nuclei by choosing the appropriate frequency of resonant cw and pulsed RF excitation. To illustrate this possibility, Fig.4c shows a calculated color-plot (all parameters as in Fig.4a,b) representing an NMR-frequency map of the dot with individual colors showing locations of nuclei with the same resonant frequency.

For a given wave-function volume the NMR frequency gradients, and hence, spatial selectivity in manipulation of nuclear spins can be enhanced even further for the case of a higher magnitude of the product ρF , as shown in Fig.4d: for $\rho F = 0.6$ the width of the resonance can be increased by a factor exceeding 7 compared with an electron-free dot ($\rho F = 0$), and by a factor of ≈ 3 compared to the case of $\rho F \approx 0.16$, observed in Fig.3. High magnitudes of ρF can be realized in an electron-doped dot in high magnetic fields at low temperatures, where $F = 1$ and ρ may also approach 1. To demonstrate further the potential for spatial selectivity, we show in Fig.4e calculated NMR curves for a mono-layer (ML) of ^{71}Ga situated 2, 6, 9 and 11 MLs (1 ML= 0.28 nm) from the the dot center in the case of an ρF factor of 0.5. A strong dependence of the resonance shapes on the ML position

is observed with pronounced broadening and asymmetric shapes for the 2 and 6 ML displacement, where the peak maxima are observed at high Knight shifts [29].

To conclude, we demonstrate optically controlled tuning of the NMR frequencies of small ensembles of nuclear spins inside a semiconductor quantum dot. We have employed strain-free GaAs/AlGaAs interface QDs, where inhomogeneities of the resonant frequencies due to the non-zero nuclear quadrupole moments are not significant, in contrast to self-assembled QDs [30]. We have been able to demonstrate tunability of the magnetic resonance in a dot, and have shown that various distributions of these resonant frequencies can be created in a controlled fashion via optical excitation of a spin-polarized electron. This has potential for precise manipulation of Overhauser fields on the nano-scale via addressing groups of only a few hundred nuclei in GaAs nano-structures with a few nm-resolution.

We thank K. V. Kavokin and A. J. Ramsay for fruitful discussions. This work has been supported by the EPSRC Programme Grant EP/G601642/1. AIT is grateful for support by an EPSRC ARF.

-
- [1] B. E. Kane, Nature **393**, 133137 (1998)
 - [2] L. M. K. Vandersypen *et al.*, Nature **414**, 883887 (2001).
 - [3] M. N. Leuenberger *et al.*, Phys. Rev. Lett. **89**, 207601 (2002).
 - [4] G. Yusa *et al.*, Nature **434** 1001 (2005).
 - [5] J. J. L. Morton *et al.*, Nature **455** 1085 (2008).
 - [6] D. J. Reilly *et al.*, Science **321**, 817 (2008).
 - [7] X. Xu *et al.*, Nature **459**, 1105 (2009).
 - [8] D. Brunner *et al.*, Science **325**, 70 (2009).
 - [9] A.I. Ekimov, V.I. Safarov, JETP Lett. **15**, 179 (1972).
 - [10] D. Paget, Phys. Rev. **B 25**, 4444 (1982).
 - [11] S. E. Barret *et al.*, Phys. Rev. Lett. **72**, 1368 (1994).
 - [12] M. Eickhoff *et al.*, Phys. Rev. **B 71**, 195332 (2005).
 - [13] J. G. Kempf, M. A. Miller, D. P. Weitekamp, Proceedings of the National Academy of Sciences, **105**, 20124 (2008).
 - [14] D. Gammon *et al.*, Science **277**, 85 (1997).
 - [15] D. Gammon *et al.*, Phys. Rev. Lett. **86**, 5176 (2001).
 - [16] S.W. Brown *et al.*, Solid State Nuclear Magnetic Resonance **11**, 49 (1998).
 - [17] Knight shifts in interface dots have been reported in Ref.[16]. However, no detailed investigation of their dependence on the power and polarization of optical excitation has been carried out.
 - [18] A. Abragam, *Principles of Nuclear Magnetism*, Oxford University Press (1961).
 - [19] C. W. Lai *et al.*, Phys. Rev. Lett. **96**, 167403 (2006).
 - [20] E. A. Chekhovich *et al.*, Phys. Rev. **B 81**, 245308 (2010).
 - [21] E. Peter *et al.*, Phys. Rev. Lett. **95**, 067401 (2005).
 - [22] B. Eble *et al.*, Phys. Rev. **B 74**, 081306(R) (2006).
 - [23] A. E. Nikolaenko *et al.*, Phys. Rev. **B 79**, 081303(R) (2009).
 - [24] A. I. Tartakovskii *et al.*, Phys. Rev. Lett. **98**, 026806 (2007).
 - [25] E. A. Chekhovich *et al.*, Phys. Rev. Lett. **104**, 066804

- (2010).
- [26] The sample is pumped with a train of 10 s pulses of circularly polarized light interrupted by 500 ms "dark" gaps. When light is switched off the dot is excited with a 500 ms RF pulse. PL is measured in the first 50 ms of each optical pulse. NMR peaks are obtained by varying the radio frequency and repeating the measurement cycle.
- [27] J.-W. Luo, G. Bester, and A. Zunger, Phys. Rev. **B 79**, 125329 (2009).
- [28] More precise knowledge on the exciton life-time and inclusion of the electron and hole spin states and their relaxation in the model will allow independent calculation of F . In that case the fitting in Fig.3 can be used for calculation on the volume of the electron wave-function.
- [29] This is in contrast to the NMR lineshape for $\rho^F = 0.5$ in Fig.4d, indicating a smaller relative contribution of nuclei in the regions with low $|\psi(\mathbf{r})|^2$ in a ML compared to the whole dot.
- [30] P. Maletinsky *et al.*, Nature Physics **5**, 407 (2009).